

Article

# MELCOR Analysis of a SPARC Experiment for Spray-PAR Interaction during a Hydrogen Release

Hyoung Tae Kim \*  and Jongtae Kim

Accident Monitoring and Mitigation Research Team, Korea Atomic Energy Research Institute (KAERI), Daeduk-daero 989-111, Daejeon 34057, Korea; ex-kjt@kaeri.re.kr

\* Correspondence: kht@kaeri.re.kr; Tel.: +82-42-868-8720

Received: 8 October 2020; Accepted: 28 October 2020; Published: 30 October 2020



**Abstract:** A series of experiments were performed in the SPARC (spray-aerosol-recombiner-combustion) test facility to simulate a hydrogen mitigation system with the actuation of a PAR (passive auto-catalytic re-combiner) and spray system. In this study, the SPARC-SPRAY-PAR (SSP1) experiment is chosen to benchmark the MELCOR (a lumped-parameter code for severe accident analysis) predictions against test data. For this purpose, firstly we prepared the base input model of the SPARC test vessel, and tested it by a simple verification problem with well-defined boundary conditions. The implementation of a currently used PAR correlation in MELCOR is shown to be appropriate for the simulation of a PAR actuation experiment. In an SSP1 experiment, the PAR is reacting with hydrogen, and the spray actuation starts as soon as hydrogen injection is complete. The MELCOR simulation well predicts the pressure behavior and the gas flow affected by operating both a PAR and spray system. However, the local hydrogen concentration measurement near the inlet nozzle is much higher than the volume average-value by MELCOR, since high jet flow from the nozzle is dispersed in the corresponding cell volume. The experimental reproduction of the phenomena we expect, or, conversely, the identification of phenomena we do not understand, will continue to support the verification of analytical models using experimental data and to analyze the impact of spray on PAR operations in severe accident conditions.

**Keywords:** severe accident; containment; hydrogen behavior; spray; PAR; SPARC test facility; MELCOR code

## 1. Introduction

In order to remove a hazard of hydrogen explosion in a nuclear power plant (NPP) containment during a severe accident, it is necessary to have a hydrogen mitigation system (HMS) installed in the containment [1]. Among hydrogen mitigation devices, passive auto-catalytic re-combiners (PAR) [2] are commonly used in nuclear reactor containments because of their passive hydrogen depletion characteristic. Addition to PARs, the spray system can be utilized to manage the hydrogen safety and prevention of over-pressurization of the containment. The spray operation in containment building may affect the behavior of hydrogen removed by PAR at the same time as the inherent goal of hydrogen removal and pressure control in the containment building [3].

The Korea Atomic Energy Research Institute (KAERI) has built a large-sized test facility, called SPARC (spray-aerosol-recombiner-combustion) [4] for an experimental simulation of HMS in the containment building. A series of experiments were performed in the SPARC test facility to simulate a PAR actuation [5] in the release of hydrogen under the steam-air mixing condition and the operation of spray system with PARs for evaluation of the effect of spray to hydrogen removal characteristics of a PAR [4].

In parallel to the experimental study, an analytical study for numerical simulations of the SPARC experiments with a PAR and spray system are performed in the present study. For this purpose, we are using a lumped-parameter (LP) analysis code, MELCOR [6,7].

In the preliminary work [8], as part of our efforts to establish a confident analysis environment, we prepared the input models of MELCOR for PAR and spray experiments which have been conducted in the SPARC test facility. For this purpose, modelling of the control volumes and flow paths for SPARC test vessel was automated by an Excel sheet to avoid user mistakes and to save time for simple recurring tasks. The base input of MELCOR was also tested by a simple verification problem with well-defined boundary conditions.

The MELCOR ESF Package models [6] the phenomena for the various engineered safety features (ESFs) in a nuclear power plant. The PAR package constitutes a sub-package within the ESF package, and calculates the removal of hydrogen from the atmosphere due to the operation of passive hydrogen reaction devices. The MELCOR code adopts the basic Fischer NIS equation form [9] as a default model and its PAR package can handle total gas volumetric flow rate and the efficiency of the PAR unit.

In the present work, five PAR correlations from each different manufacturer were identified and the parameters in each PAR correlations were captured by various control functions of the MELCOR code. Finally, a simple verification test for PAR actuation in the single volume of the MELCOR was performed. The hydrogen removal results of MELCOR code with these five PAR correlations were compared with each other.

The containment spray system is an important means of preventing overpressure through depressurization of the containment atmosphere, and is used to manage both design basis accidents and severe accidents [10].

The spray system controls the pressure by reducing the temperature and inducing condensation of water vapors through heat transfer with the atmosphere in the containment building [11]. At this time, the concentration of hydrogen may increase relatively as the concentration of water vapor decreases due to condensation. Conversely, the behavior of the spray droplet is caused by the friction at the liquid interface, which results in the exchange of momentum between the droplet and surrounding atmosphere, thereby increasing the stratified mixture of hydrogen. Therefore, the spray operation in the containment building has a significant impact on the distribution and behavior of hydrogen, so it is important to evaluate the spray operation in terms of hydrogen control in severe accidents.

Experimental and analytical studies have been conducted or in progress on the effects of spray on condensation of water vapor, hydrogen mixing, hydrogen combustion, etc. [12–18]. The purpose of the spray test is to investigate the thermal hydraulic behavior of the containment atmosphere with spray operation, especially the behavior of hydrogen and fission product aerosols in the event of severe accidents. The safety issues of spray experiments related to the behavior of hydrogen are various, including the mixing characteristics of hydrogen by the spray liquid, the distribution of hydrogen by the condensation of water vapor, and the propagation characteristics of hydrogen flame by the spray.

The SPARC spray experiments [4,10] were performed to simulate two main phenomena. The SPARC-SPRAY (SS) experiment is to assess the effect of spray on the distribution of hydrogen with spray actuation while hydrogen is released, and the SPARC-SPRAY-PAR (SSP) experiment is to investigate the effect of spray on the operation of PARs.

In the SPARC spray experiment, the size of the spray droplet (300  $\mu\text{m}$  in diameter) and average nozzle flow rate (1 kg/s) are chosen as the equivalent factors for actual plant (APR1400 [16]). However, the free volume of SPARC is not so enough to maintain the spray injection angle of  $60^\circ$  for APR1400. Instead, the spray injection angle of  $30^\circ$  is selected to prevent spray fluid from falling onto the upper outlet surface of the PAR installed in the SPARC test vessel. Thus, it may simulate only a well-defined condition for specified issue phenomenon. However, SPARC spray experiments can contribute to providing experimental data for understanding the hydrogen issue phenomena and the verification of analytical models associated with the operation of pressure control devices in the containment building.

The SPARC-SPRAY-PAR (SSP1) experiment is simulated by MELCOR 1.8.6 in the present study. The MELCOR Containment Sprays (SPR) package [7], which calculates the thermal-hydraulic behavior associated with spray systems, models the mass and heat transfer rates between spray droplets and control volumes. With the MELCOR analysis of a spray experiment, the containment analysis code can be assessed to remove the uncertainties of the code models regarding spray actuation phenomena in the containment.

## 2. Facility and Test Description

### 2.1. SPARC Test Facility

#### 2.1.1. Test Vessel

SPARC (spray-aerosol-recombiner-combiner-combination), a scaled-down test facility of a simulated containment building, has a pressure vessel capable of controlling the temperature of 82 m<sup>3</sup> volume. Figure 1 shows the configuration of the SPARC test facility and its geometric size. The pressure vessel is 3.4 m in diameter and 9.76 m in height. Table 1 lists the design specifications of the test vessel.

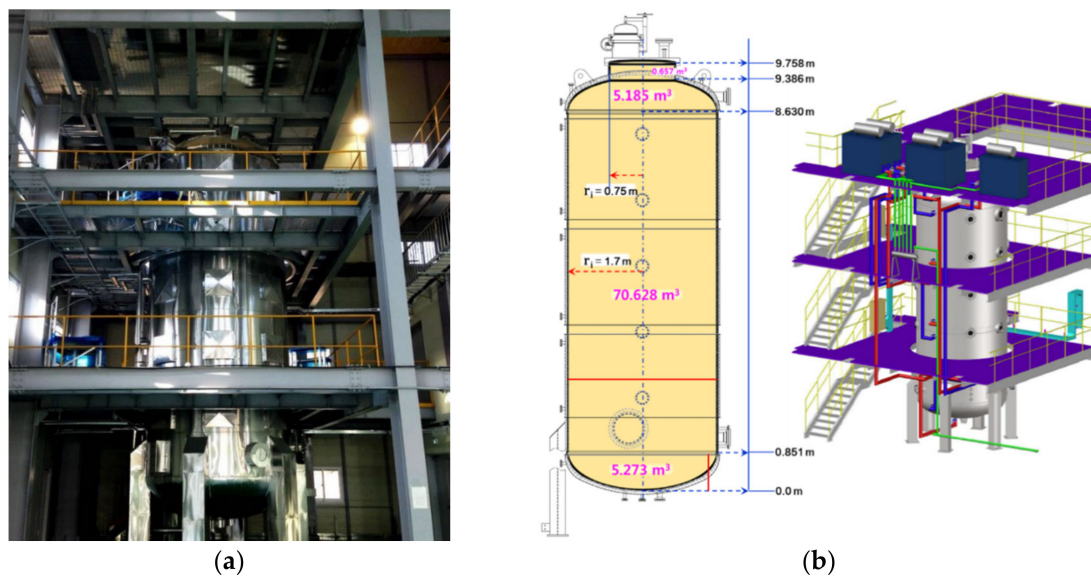


**Figure 1.** Configuration of the SPARC test facility: (a) Overall view of test apparatus; (b) Geometric dimension of the SARC test vessel.

**Table 1.** Design specifications of the test vessel.

| Design Parameter    | Value, Specification  |
|---------------------|---|
| Pressure            | 15 bar (at 180 °C)  |
| Height              | 9.76 m  |
| Diameter            | 3.4 m   |
| Free volume         | 82 m <sup>3</sup>   |
| Wall heating        | Oil heating (partly electrical heating)   |
| No. of measurements | 14 (H <sub>2</sub> ), 4 (O <sub>2</sub> ), 4 (H <sub>2</sub> O), 112 (wall temperature) |

The temperature of the SPARC pressure vessel is basically controlled by an oil jacket installed on the outer wall of the pressure vessel, an oil heater, and an oil pump. There are several view ports for experimental measurement and visualization of the pressure vessel, which prevents the outer wall of the pressure vessel from being completely covered with an oil jacket. Therefore, additional electric heaters are installed for some parts of outer walls without an oil jacket.

### 2.1.2. Steam Supply System

The amount of steam supplied to the SPARC experimental vessel was estimated based on the vertical jets of steam in the helium-air stratification and mixing experiments. The Reynolds number of 20,000 is assumed from the steam injection conditions of the conventional large scale hydrogen test facility, which requires an internal diameter of 100 mm of steam jet nozzles and a steam flow rate of 68 kg/h with velocity of 4.04 m/s.

To prevent condensation in the steam injection pipe, heating tape is attached to the outer wall of the pipe so that the temperature can be kept above 100 °C.

A mass flow meter and motor-driven valve are installed to control the steam flow rate. The mass flow control is performed by the DAS program.

### 2.1.3. Non Condensable Gas Supply System

Non condensable gases used in the SPARC experiment are air and hydrogen gases.

- Air

Compressed air of 6–7 bar is supplied to the test building where the pressure vessel is installed. The compressed air was connected to the inlet nozzle of the vessel through a 3/4 inch stainless steel pipe. In addition, the air compressor and receiver tank are installed to provide a stable air supply. The air supply piping is equipped with a vortex flowmeter to measure the flow rate. The time required to fill the pressure vessel (82 m<sup>3</sup>) up to 5 bar is calculated to be approximately 3 h

- Hydrogen

Since hydrogen is a combustible gas, it is built so that it can be stored and supplied independently of other gases (air). Piping for hydrogen supply is connected by welding with minimal fitting to prevent possible gas leakage at the connecting part. VCR (Vacuum Coupling Radiation) fitting is used for parts that need to be replaced, such as flowmeter installed in piping. The hydrogen pressure is adjusted by a regulator at the hydrogen Bombay reservoir installed outside the test building. Flame Arrestor and a flow meter (VAF-M3, Swagelok), and explosion proof solenoid valves were installed inside the test building. The flow meter measures 0–100 L/min.

## 2.2. Measurements

### 2.2.1. Temperature

In the SPARC experiment, wall temperature control and gas temperature measurement are very important factors. The thermocouples are installed at various locations on the wall of the experimental vessel to measure the temperature distribution of the wall and evaluate the heat loss outside the wall. It used a thermocouple (CO3-K, OMEGA, K-type, internal diameter of 0.25 mm bead, 300 ms) that is easy to attach to the curved walls of the vessel with an epoxy of high thermal conductivity and operating temperature (OB-200-2, OMEGA, 1.38 W/m-K, operating temperature 260 °C).

The thermocouple installed on the inner wall of the vessel is connected to the data acquisition system outside the vessel through feed-through (PFTFS-8K, OMEGA, leakage rate of  $1 \times 10^{-7}$  cc air/s at maximum pressure of 138 bar, and connection line diameter of 0.812 mm).

For gas temperature measurements to be compared with MELCOR simulation, in this study, the thermocouples are located at the same points for the hydrogen concentration measurement as shown in Figure 2.

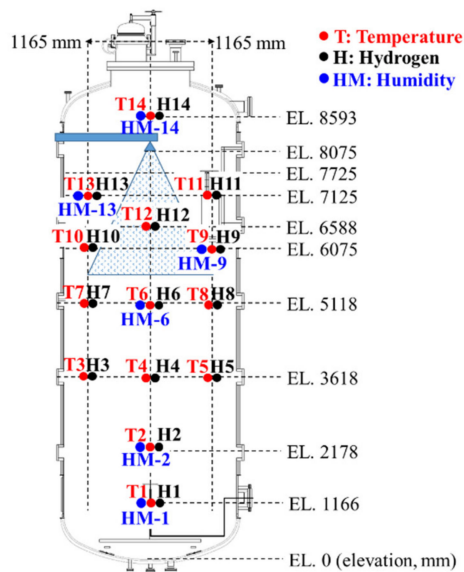


**Figure 2.** Arrangement of gas temperature, hydrogen, and humidity sensors for SPARC spray test [10].

### 2.2.2. Gas Concentration

The distribution of hydrogen concentrations inside the test vessel can be selected from various methods. The SPARC and THAI [15] test apparatus use a thermal conductivity sensor, while the PANDA, MISTRA, and CIGMA test apparatus [12] measure the concentration of hydrogen by sampling gas at a specific location inside the vessel using a mass spectrometer. There are 14 hydrogen concentration sensors as shown in Figure 2.

### 2.2.3. Humidity

Since steam is a condensed gas, a probe-type humidity meter is installed so that humidity can be measured directly inside the SPARC test vessel rather than by sampling method.

There are 6 relative humidity sensors installed in the SPARC test facility. The detail specifications of the sensors are described in the reference [4]. The locations of the sensors can be changed for difference test cases. The arrangement of the concentration measurement sensors for the SPARC spray test are shown in Figure 2.

### 2.3. PAR

In the SPARC-PAR experiment, two small size model of PARs, KPAR-40 from Korea Nuclear Technology, Inc. (KNT) [19], are installed at an elevation of 6 m from the bottom of the SPARC vessel. Figure 3 shows the configuration of the KPAR-40 installed in the SPARC test facility.

The KNT PAR [20] has a structure of box made of a stainless steel, and the catalysts are installed at the bottom of the box. Air is taken in from the entrance at the bottom of the PAR. The upper part of box is open in three directions for exit flow and the heat generated in the lower part by the catalytic reaction can drive a natural circulation flow due to the chimney effects. The cross sectional area at the PAR exit is larger than that of catalysts. The catalyst of KNT PAR is the honeycomb type, and the support structure is made of a Cordierite ( $2\text{MgO}\cdot 2\text{Al}_2\text{O}_3\cdot 5\text{SiO}_2$ ) ceramic material. It is coated with Aluminium oxide ( $\text{Al}_2\text{O}_3$ ) sol and chloroplatinic acid ( $\text{H}_2\text{PtCl}_6\cdot n\text{H}_2\text{O}$ ). The dimensions of the honeycomb type catalyst support are  $15 \times 15$  cm with the height of 5 cm.

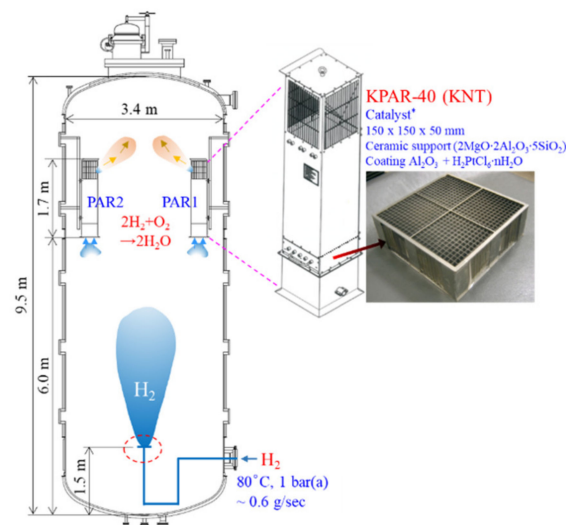


Figure 3. PARs installed in the SPARC test vessel (for the PAR experiment: SP1).

#### 2.4. Spray System

The spray of SPARC test facility is designed in accordance with the specifications of the spray system installed in APR1400 [16,21]. The spray nozzle of APR1400 is the hollow cone type, with an average flow rate of 1 kg/s per nozzle and a volume-average droplet size is approximately 300  $\mu\text{m}$  in diameter. In the APR1400 containment building, about 300 main spray nozzles per train are installed and the height of the dome to the work deck is more than 40 m. Therefore, the spray droplets from the hollow cone type nozzles are impinging on the bottom surface with an almost a packed circle, which is simulated by a full cone type spray nozzle in the SPARC spray tests. The spray injection angle of 30° is selected to prevent spray fluid from falling onto the upper outlet surface of the PAR installed in the SPARC test vessel.

To evaluate the performance of the spray nozzle with the current design, droplet size distribution, droplet ejection angle, and impinging area on the bottom surface, performance tests with specified operation conditions are performed. Figure 4 shows the droplet size distribution measured in the performance tests, where we can confirm that a volume-average droplet size is approximately 300  $\mu\text{m}$  in diameter.

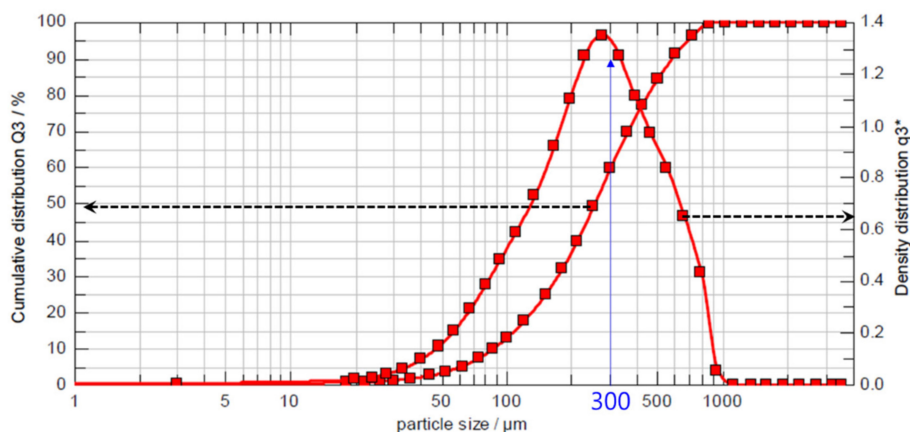
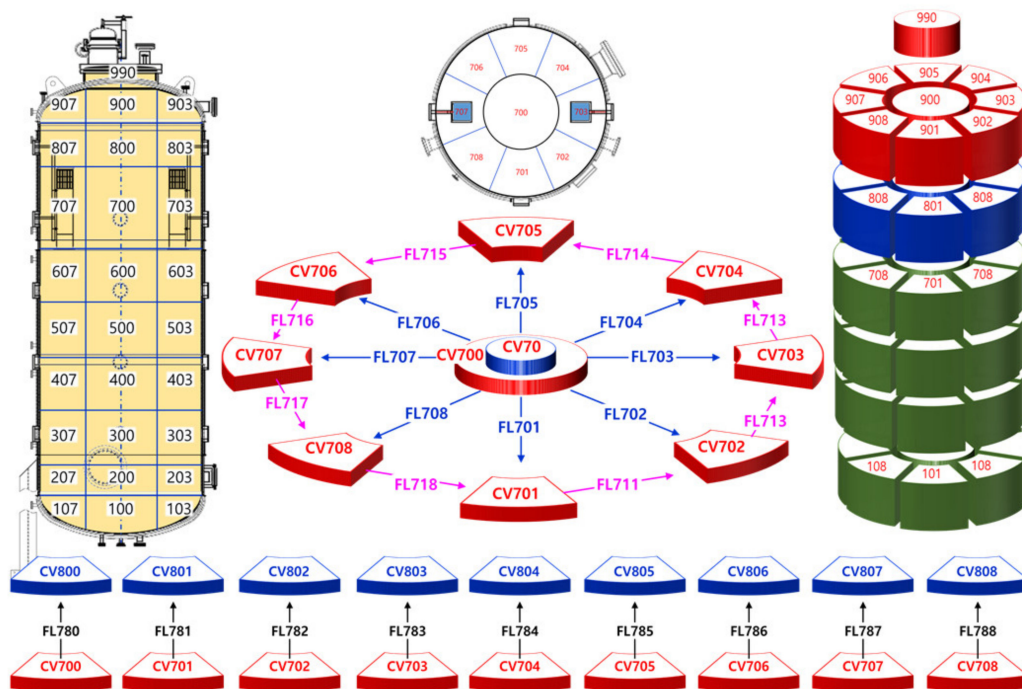


Figure 4. Size distribution of spray droplets from performance tests [4].

### 3. MELCOR Input Model

#### 3.1. Preparation of Base Input Model

MELCOR 1.8.6 was used for the analysis of SPARC tests. The geometry of test facility was modeled with 82 control volumes (CVs). Figure 5 shows the conceptual diagram for structure of CVs in this work.



**Figure 5.** MELCOR nodalization scheme for base input of SPARC test vessel.

Since most of measurement devices within test vessel are arranged with 8 circumferential segments, we divided 8 circumferential segments with one core volume in the center for each axial position. The test vessel was divided into 9 levels by elevation, which can be adjusted for cases of the simulations. The change of nodalization can be efficiently performed by an automation process using Excel sheet.

In the SPARC-PAR experiment, two small size model PARs of KNT are installed at an elevation of 6 m from the bottom of the SPARC vessel, so two PARs will be located at the CV703 and CV707, respectively. These two control volumes can be subdivided according to the detailed configuration of the PARs in the sensitivity studies.

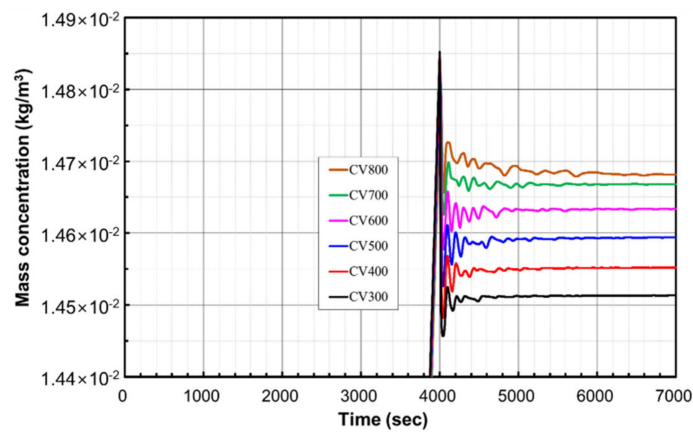
The open boundaries of each CV were modeled with 219 flow paths to the adjacent CVs along radial, circumferential, and axial (vertical) directions.

#### 3.2. Verification Test for Base Input

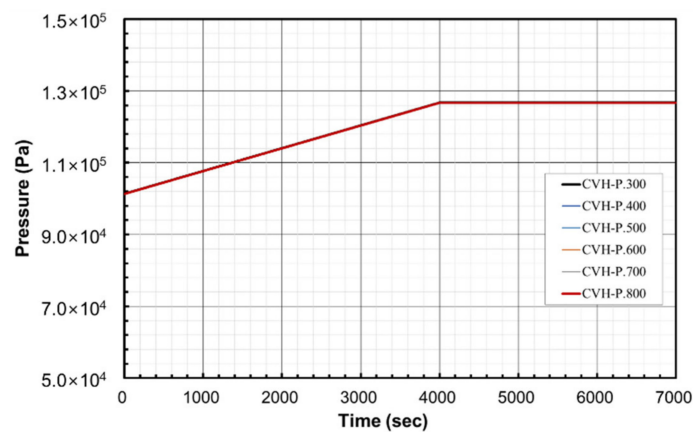
To verify the suitability of the current MELCOR input, a test calculation with well-defined steady-state conditions is performed. The minimum and the maximum time step used are 0.001 s and 0.3 s, respectively. Non-equilibrium option was used for the control volumes. A PAR package model of MELCOR is not used in this test calculation.

As a test condition, hydrogen is released for 4000 s at a rate of 0.296 g/s through a CV100. From a conventional test conditions of SPARC-PAR experiment, atmospheric air with temperature of 80 °C is initially filled in the test vessel. After stopping a cold hydrogen (30 °C) injection, it is expected that the stratification of hydrogen in the test vessel and thermal hydraulic properties of hydrogen gas will be in the steady-state.

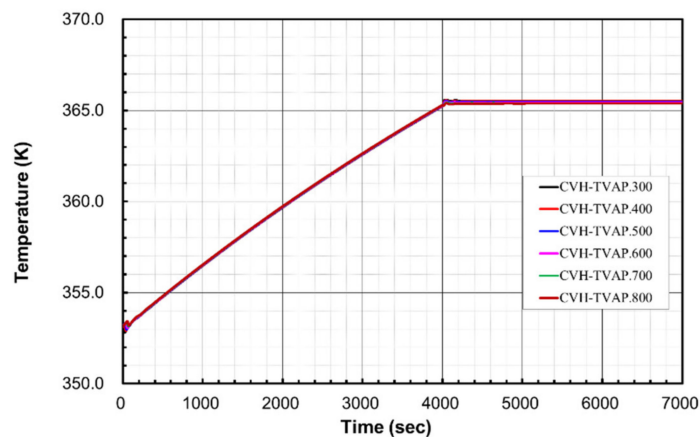
Figure 6a shows the distribution of hydrogen mass concentration along the elevation. As we expected the hydrogen is vertically stratified above more heavy gas of air. It is also shown that this distribution of mass concentrations becomes stabilized after 4000 s when injection stops.



(a)



(b)



(c)

**Figure 6.** Verification test results by base MELCOR input: (a) H<sub>2</sub> mass concentration; (b) Gas pressure; (c) Gas temperature.

Since the venting system from the test vessel is closed during the simulation, the gas pressure in the test vessel is increased as the gas is injected. Figure 6b shows the pressure increase during hydrogen injection and approach to the steady-state condition after injection stops. The gas temperature was also predicted as shown in Figure 6c. The compression of the gas in the closed volume results in an increase of the temperature following the ideal gas law.

### 3.3. Implementation of PAR Correlations

Present commercially available PARs which provide the different hydrogen depletion correlations are implemented to an input of the MELCOR PAR package. The domestic and foreign vendors of PAR are as follows:

- Korean vendors: a KNT PAR [19,20] with honeycomb shape and a CERACOM PAR [22]
- Other vendors [23,24]: a box-type PAR of AREVA (France) [25] and Atomic Energy Canada Limited (AECL, Canada) [26], and a porous bed type PAR of NIS Company (Germany)

In the present work 5 PAR correlations for each manufacturer are identified and the parameters in each PAR correlations could be captured by various control functions of the MELCOR code. Finally, a simple verification test for PAR actuation in the single volume of the MELCORE is performed. The hydrogen removal results of MELCOR code with these 5 PAR correlations are compared with each other.

#### 3.3.1. KNT PAR

KNT PAR adopts the shape of a honeycomb to create a greater catalyst surface area and an enhancement of the buoyancy-induced convective flow. The generic form of the hydrogen depletion rate,  $R$  (kg/s) by a KNT PAR is as follows:

$$R = 0.66 \times n \times (a_1 + a_2 + x_{h2} + a_3 \times x_{h2}^2) \times \left(\frac{P}{T}\right) \times 10^{-3} \left[\frac{\text{kg}}{\text{s}}\right], \quad (1)$$

where:

$n$ : multiplication factor for the size of PAR in Table 2

Values of constant parameters:

$a_1 = 2.9193$ ,  $a_2 = 9.0852$ ,  $a_3 = 2.3392$

$x_{h2}$ : hydrogen concentration (vol. %)

$p$ : pressure (bar)

$T$ : temperature (K)

**Table 2.** Multiplication factor for different size of KNT PAR.

| KNT Model | $n$ Value |
|-----------|-----------|
| KPAR-40   | 1         |
| KPAR-80   | 2         |
| KPAR-160  | 4         |

#### 3.3.2. CERACOM PAR

The generic form of the correlation for CERACOM PAR is as follows:

$$R = k \times x_{h2}^{1.1} \times P^{1.2} \left(\frac{273}{T}\right)^{1.5} \times 10^{-3} \left[\frac{\text{kg}}{\text{s}}\right], \quad (2)$$

where:

$k$ : multiplication factor for the size of PAR in Table 3

$x_{H_2}$ : hydrogen concentration (vol. %)

$p$ : pressure (bar)

**Table 3.** Multiplication factor for different size of CERACOM PAR.

| CERACOM Model  | $k$ Value |
|----------------|-----------|
| NP400 (small)  | 0.05      |
| NP800 (medium) | 0.106     |
| NP1600 (large) | 0.255     |

### 3.3.3. AECL PAR

The generic form of the correlation for AECL PAR is as follows:

$$R = 0.2778 \times 10^{-3} \times (0.15196 \times x_{H_2} + 0.0126 \times x_{H_2}^2) \times \left(\frac{298}{T}\right)^{1.10974} \times P^{0.57769} \left[\frac{\text{kg}}{\text{s}}\right], \quad (3)$$

where:

$x_{H_2}$ : hydrogen concentration (vol. %)

$p$ : pressure (bar)

$T$ : temperature (K)

### 3.3.4. AREVA PAR

The generic form of the correlation for AREVA PAR is as follows:

$$R = n x_{min} (A \times P + B) \tanh(100 x_{min,lim}) \times 10^{-3} \left[\frac{\text{kg}}{\text{s}}\right], \quad (4)$$

where

$$n = \begin{cases} 1, & x_{H_2} \leq x_{O_2} \\ 0.6, & x_{H_2} > x_{O_2} \end{cases}$$

$x_{H_2}$ : hydrogen concentration (–)

$x_{O_2}$ : oxygen concentration (–)

$x_{min}$ :  $\min(x_{H_2}, 2.0 \times x_{O_2}, 0.08)$   $x_{min,lim}$ :  $\max(x_{min} - 0.005, 0.0)$

$p$ : pressure (bar)

$A, B$ : constant parameters for PAR models in Table 4

**Table 4.** Values of constant parameters for AREVA PAR.

| AREVA Model | A    | B    |
|-------------|------|------|
| FR1-380T    | 3.1  | 3.7  |
| FR1-750T    | 6.1  | 7.4  |
| FR1-1500T   | 13.7 | 16.7 |

### 3.3.5. NIS PAR

The generic form of the correlation for NIS PAR [8] is as follows:

$$R = 0.85 \rho_{H_2} \times 0.67 x_{H_2}^{0.307} = 1.134 \times x_{H_2}^{1.307} \frac{p}{R_u T} \left[\frac{\text{kg}}{\text{s}}\right], \quad (5)$$

where:

$\rho_{H_2}$ : hydrogen density ( $\text{kg/m}^3$ )

$x_{H_2}$ : hydrogen volume concentration (–)

$p$ : pressure ( $\text{kg/m}^2\text{-s}^2$ )

$R_u$ : universal gas constant = 8314 (J/kmol-K)

### 3.4. Verification Tests for Implementation of PAR Correlations

The MELCOR code adopts the basic Fischer NIS equation form [9] as a default model and its PAR package can handle total gas volumetric flow rate ( $\text{m}^3/\text{s}$ ) and the efficiency of the PAR unit. Therefore, the final output of control function should be the PAR correlation values divided by the hydrogen density ( $\text{kg/m}^3$ ) in the specified volume occupied by the PAR devices.

The single volume is defined and a constant flow rate of  $\text{H}_2$ , 0.262 g/s is maintained for 1000 s. Two PARs are assigned to the single volume for each simulation.

The pressure and temperature of injection flow is 1 bar and 30 °C, respectively.

For the type of the PARs, the small size is selected as: KNT (KPAR-40), CERACOM (NP400), and AREVA (FR1-380T).

Figure 7 shows the amount of the hydrogen in the volume of MELCOR when different PAR models are applied to the code. As we assumed the flow boundary condition, the cumulative mass of hydrogen for 1000 s is 0.26 kg. Since the hydrogen injection flow rate is higher than the depletion rate by PARs, it shows the peak value of the hydrogen inventory when the injection flow ends at 1000 s. NIS PAR has the highest performance for hydrogen depletion and the second performance by AREVA PAR. The other three PARs, namely KNT, AECL, and CERACOM, show similar performance.

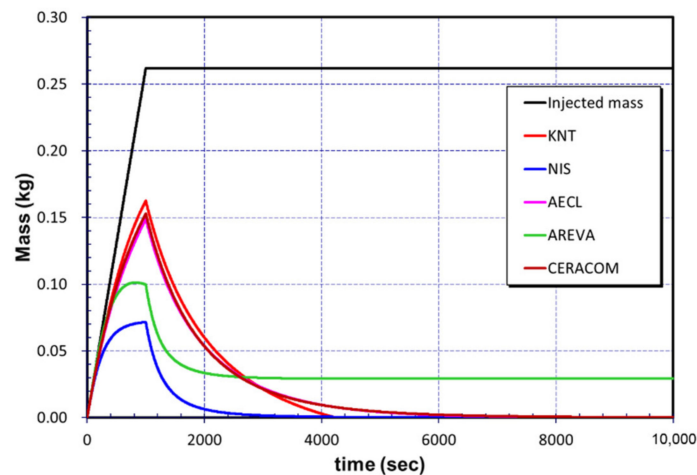


**Figure 7.** Comparison of the PAR performances (hydrogen inventory) by different manufacturer's correlations.

From verification test of the implementation of PAR correlations, it is shown that each PAR correlations are well implemented to the MELCOR and the characteristics of each PARs can be compared with each other. The removal of hydrogen by the KNT PAR correlation is implemented the MELCOR input to simulate the SSP1 experiment in the following section.

## 4. MELCOR Analysis of a SPARC-SPRAY-PAR Experiment

### 4.1. SPARC-SPRAY-PAR Experiments

The SPARC spray experiments were performed to simulate two main phenomena. The SPARC-SPRAY (SS) experiment is to assess the effect of spray on the distribution of hydrogen with spray actuation while hydrogen is released, and the SPARC-SPRAY-PAR (SSP) experiment is to investigate the effect of spray on the operation of PAR.

In the SS experiment with the spray actuation under water vapor conditions, the distribution and behavior of helium were investigated by injecting water vapor and helium (hydrogen substitute gas) into the test vessel. Although the spray can increase the concentration of helium by inducing condensation of water vapor, it was observed that the distribution of helium becomes almost uniform by mixing of helium due to strong turbulence flow induced by the behavior of the spray liquid.

The SSP experiment is supposed to investigate how spray affects the operation of PARs. Various factors can affect the influence of the spray and PAR. Among a series of SSP experiments, the SSP1 and SSP2 experiments are distinguished by the actuation time of the spray.

The experiments are carried out step by step as shown in Figure 8. In phase 0 (initial step), the air temperature in the test vessel is raised up to 120 °C under atmospheric pressure condition and in phase 1 the water vapor is injected into the test vessel to build up the inner pressure to about 2.0 bar. In phase 2, the spray is activated at the same time (SSP2) or after (SSP1) hydrogen is injected into the vessel.

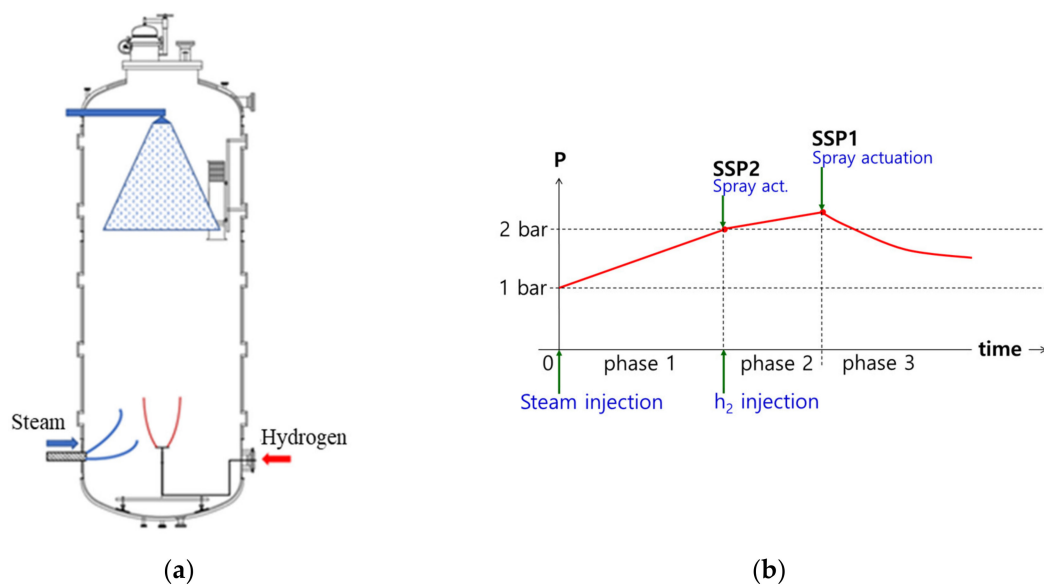


**Figure 8.** SPARC-SPRAY-PAR (SSP1) experiment: (a) Configuration of flows inside vessel; (b) Test conditions step by step.

#### 4.2. MELCOR Modeling of SSP1 Test

In the MELCOR spray simulation, the droplets heated up and cooled down by MELCOR spray system model are circulated by forced convection flow. Therefore, heat and mass transfer rates are calculated by forced convective heat transfer coefficient. The final droplet mass and temperature are calculated numerically using the Runge–Kutta method by integrating heat and mass transfer rates over the fall height of the spray droplet. Total heat and mass transfer rates are obtained by multiplying the rates for one droplet by the total number of droplets with the same size and summing over all droplet sizes. The droplet size is calculated by its temperature and height on each occasion as shown in Equations (6)–(8). Also, these droplets are assumed to be spherical and isothermal.

$$\frac{dm}{dt} = -2\pi\rho_g D \left(1 + 0.25 Re^{\frac{1}{2}} SC^{\frac{1}{3}}\right) D_c \ln(1 + B) \quad (6)$$

$$\frac{dT}{dt} = \frac{1}{mC_{pl}} \left[ \frac{C_{pv}(T - T_{cv})}{(1 + B)^{1/Le} - 1} + h_{fg} \right] \frac{dm}{dt} \quad (7)$$

$$\frac{dz}{dt} = \left[ \frac{4(\rho_d - \rho_g)gD}{3\rho_g C_d} \right]^{1/2} \quad (8)$$

where:

$m$  = droplet mass (kg),

$T, T_{cv}$  = droplet, control volume atmosphere temperatures (K),

$z$  = droplet fall height (m),

$\rho_d, \rho_g$  = droplet, atmosphere densities (kg/m<sup>3</sup>),

$c_{pl}$  = droplet specific heat capacity (J/kg-K),

$c_{pv}$  = control volume atmosphere specific heat capacity (J/kg-K),

$h_{fg}$  = latent heat of vaporization (J/kg),

$D$  = droplet diameter (m),

$Re$  = Reynolds number,

$Sc$  = Schmidt number,

$Le$  = Lewis number,

$D_c$  = diffusion coefficient (m<sup>2</sup>/s),

$C_d$  = drag coefficient, and

$B$  = the mass transfer driving force ( $n$ )

In this study SSP1 test is chosen for simulation by the MELCOR 1.8.6 to compare the code results with experimental data. In SSP1 test, as the injection of hydrogen initiates the PAR actuation, the exhaust gas including hot water vapor is released at exit of PAR. The PAR chamber produces a flow that is raised by the chimney effect and the incoming flow is created at the entrance of the PAR. Operation of the spray may interfere with the flow induced by the PAR by lowering the temperature of the exhaust gas and condensing the water vapor contained in the exhaust gas. Conversely, a downward flow driven by a spray droplet may produce a positive effect on the gas flow inside the PAR by raising the gas flow surrounding the PAR.

MELCOR input nodalization for the SSP1 test is adjusted to account for installation of the spray system, a PAR, hydrogen concentration, gas in flow rate at inlet of PAR, temperature, and pressure measurement sensor. MELCOR spray model package [27] suitable to the experimental conditions are adopted. Experimental procedures and test conditions are summarized according to time history of the spray test, and based on it, the basic boundary conditions of the MELCOR input are set as follows in Table 5.

**Table 5.** Test procedures and boundary conditions applied to MELCOR input.

| Time (s) | Test Procedures                 | Test Conditions/MELCOR Input  |
|----------|---------------------------------|---|
| 1420     | Steam injection starts          | pressure: 1.0 bar temperature: 126 °C mass flow: 0.0264 kg/s          |
| 3130     | End of steam injection          |   |
| -        | Steady conditions               |   |
| 5675     | H <sub>2</sub> injection starts | temperature: 27 °C flow: ~60 LPM                                      |
| 6680     | End of H <sub>2</sub> injection |   |
| 6709     | Spray starts                    | temperature: 52.7 °C flow: 0.197 × 10 <sup>-3</sup> m <sup>3</sup> /s |
| 11,609   | End of spray actuation          |   |

Heat structures capable of simulating heat losses on the outer walls of the test vessel are modeled. In particular, the temperature boundary condition is properly given to the outer wall and the heat transfer coefficient boundary condition is set on the inner wall to compensate for the pressurization and temperature rise conditions of the internal vessel due to the injection of steam and hydrogen. Heat structure boundary conditions for the MELCOR simulation, which can control the heat loss, are shown in Table 6.

**Table 6.** Heat structure boundary conditions (for heat loss of outer wall of the test vessel).

| Parameter   | Value   |
|---|---|
| Thickness (mm)  | 25  |
| $C_p$ (heat capacity of wall, J/Kg/K)                 | 510   |
| $\rho$ (wall density, J/kg/K)                         | 7970  |
| $k$ (conductivity, W/m/K)                             | 15  |
| Heat transfer rate on the inner surface ( $W/m^2/K$ ) | 1. Steam injection: 8.0<br>2. H <sub>2</sub> injection: 100.0<br>3. Steady state: 20.0<br>4. Spray actuation: 100.0 |
| Outer wall temperature (K)                            | 399.15  |

For comparison of code predictions with measurement data, 14 measurement points (see Figure 2) in accordance with MELCOR node are identified as shown in Figure 9a.

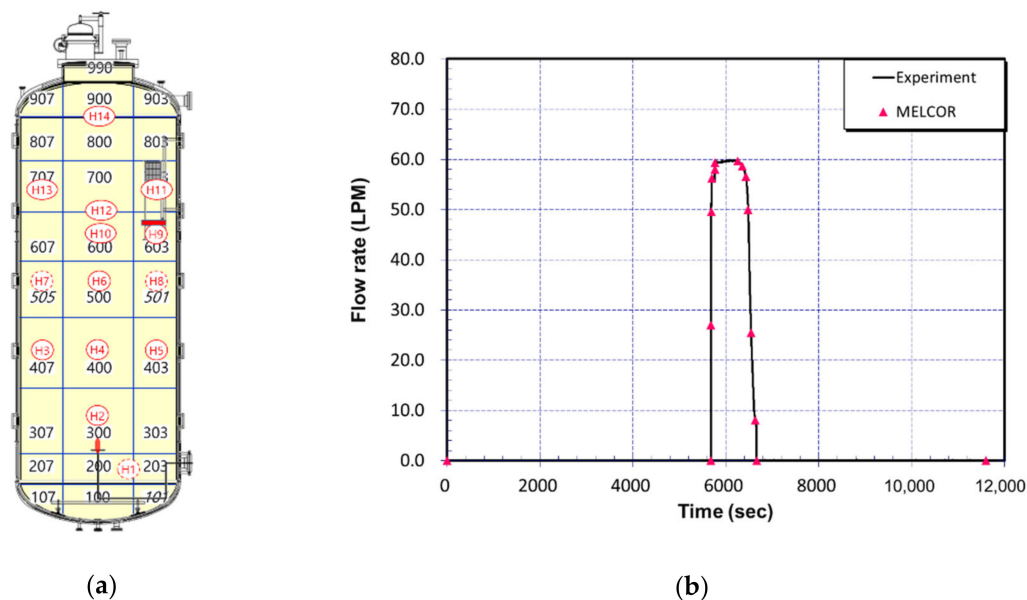


**Figure 9.** Preparations for comparison of code predictions with test data: (a) Measurement locations in accordance with MELCOR node; (b) Hydrogen injection flow data applied to MELCOR input.

The change in hydrogen flow rate injected into the SPARC vessel is sensitive to pressure changes and, in order to accurately reflect this, the measured hydrogen flow data are fitted and reflected in the MELCOR flow boundary conditions as shown in the Figure 9b.

#### 4.3. MELCOR Analysis Results of SSP1 Test

Following the procedures in the SSP1 experiment, the steam is injected approximately for 1600 s, the pressure rises from 1.0 bar to 2.0 bar. After about 3000 s of stabilization, hydrogen is injected for about 1000 s, which causes the SPARC vessel to be pressurized. The spray system is actuated to de-pressurize the vessel as soon as hydrogen injection is completed. The results of the MELCOR analysis are compared with the test results in the Figure 10.

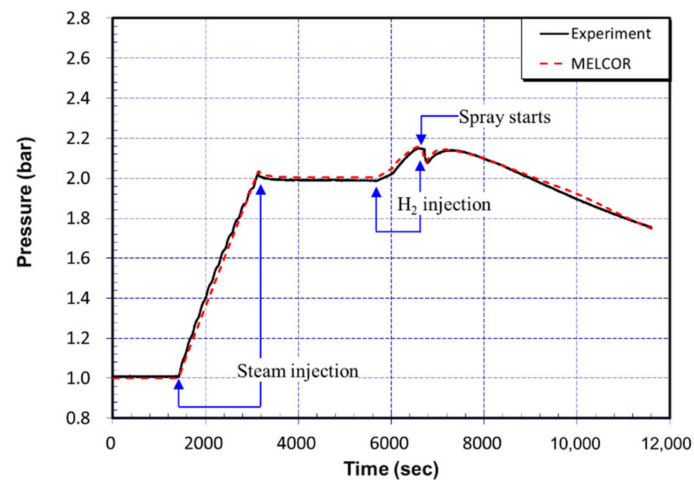


**Figure 10.** Comparison of gas pressure inside the test vessel between SSP1 test data and MELCOR prediction.

The results of the MELCOR analysis reflected the following characteristics of the test results.

- Linear pressure increase due to constant water vapor injection (1.0 bar → 2.0 bar)
- Variation of pressure increase due to hydrogen injection (with an appropriate heat loss and accurate data fitting for injection flow rate)
- Rapid de-pressurization as soon as spray injection starts, and subsequent re-rising and moderate decrease of pressure.

The test result shows that the hydrogen removal rate of PAR is affected by the operation of spray. By mixing the released hydrogen quickly, the spray reduces the concentration of hydrogen flowing into the inlet of the PAR, resulting in a relatively low hydrogen recombination rate. A temporary increase of pressure (re-rising of pressure in Figure 10) after spray actuation is due to decrease of hydrogen recombination rate.

During the hydrogen injection period, natural circulation flow of the mixture of hydrogen and steam is formed due to the operation of the PAR. The Figure 11 compares the vane flow meter reading at the PAR inlet with the MELCOR prediction at the flow path of corresponding cell connections. Since measurement of the vane flow meter has the low limit of velocity value of 0.4 m/s, the MELCOR prediction value is very similar to the experimental result except the velocity perturbation measurement of 0.4 m/s or less, which is observed prior to the start of hydrogen injection (5.75 s).

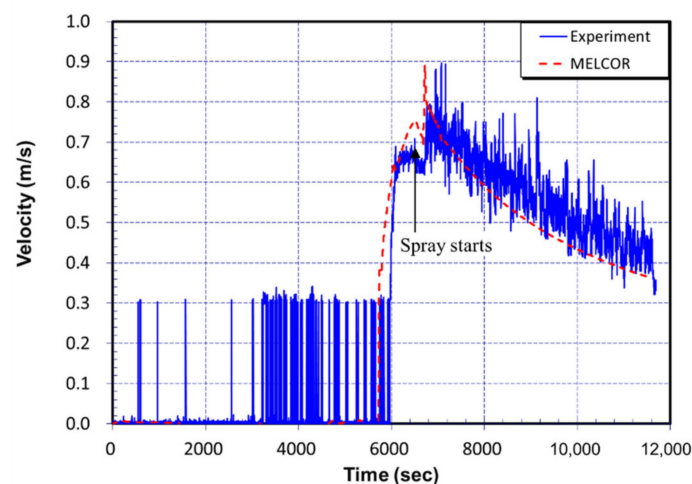


**Figure 11.** Comparison of PAR inlet flow between SSP1 test data and MELCOR prediction.

MELCOR analysis results are in well agreement with maximum velocity of hydrogen mixture gas, approximately 0.8 m/s, and also the behavior of velocity change as follows:

- Characteristic of rapid increase in inflow velocity following the start of the PAR operation after hydrogen injection.
- Temporal increase of the natural circulation flow due to rapid cooling of upper gas field at the beginning of spray injection.
- Gradual reduction of PAR inlet flow rate due to reduction of hydrogen/PAR reaction and internal temperature differences during the spray injection.

Figure 12 compares the behavior of the temperature change in the test results with that of the MELCOR analysis. The predictions of MELCOR are well in agreement with the following characteristics of the test results.

- Increase of gas temperature in the SPARC vessel by injection of steam and recover of temperature (126 °C) during stabilization period.
- Rapid increase of gas temperature inside of the vessel due to PAR operation with hydrogen injection started.
- Rapid temperature decrease immediately after spraying and subsequent behavior of mild temperature decrease.

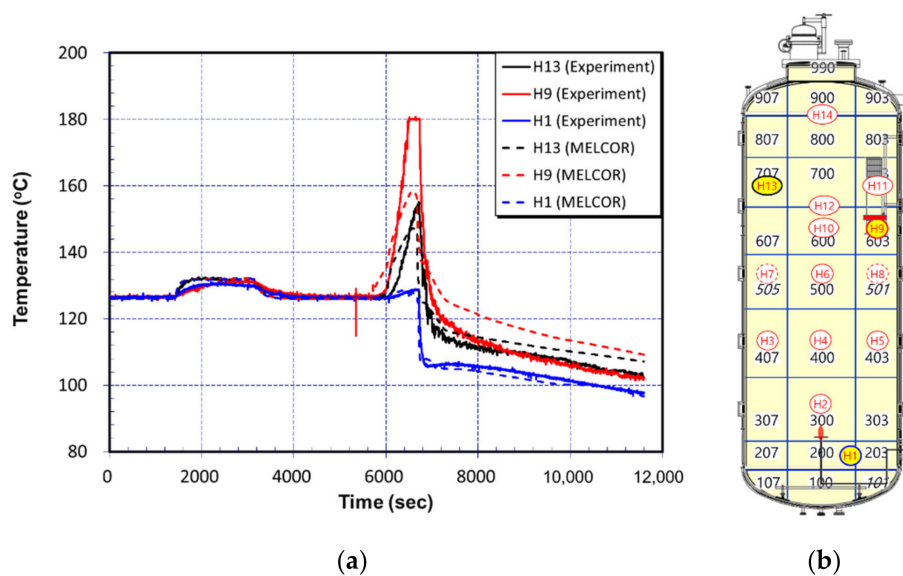


**Figure 12.** Comparison of MELCOR predictions with measurement data for SSP1 test: (a) Gas temperature; (b) Measurement locations.

Figure 13 shows the behavior of relative humidity, which is defined as the ratio of water vapor partial pressure present in a gas to the saturation vapor pressure of water at that temperature. Comparing the relative humidity measurement values with the MELCOR predictions, the trend of relative humidity change is generally well simulated. However, the MELCOR predictions are different from the experimental results in the following:

- Due to the presence of spraying droplet, local humidity measurements are higher than the MELCOR predictions (especially in areas where the liquid droplet falling down).
- As spraying droplet is accumulated at low bottom elevation (CV100) of the SPARC vessel after about 10,000 s, MELCOR code predicts that water vapor partial pressure is decreasing, while the saturation vapor temperature rarely changes. Therefore, humidity calculation values drop, although the humidity measurement (HM1) is still 100%.

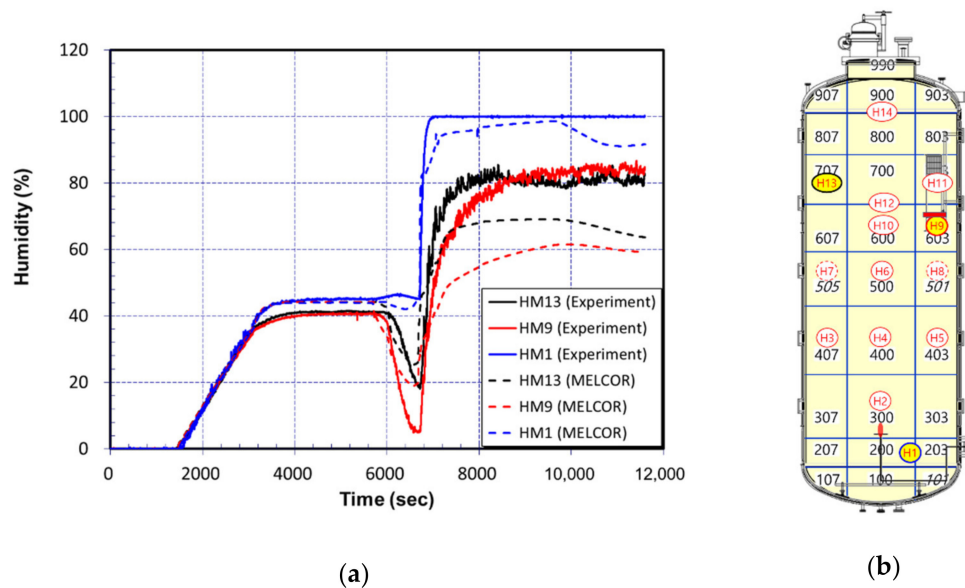
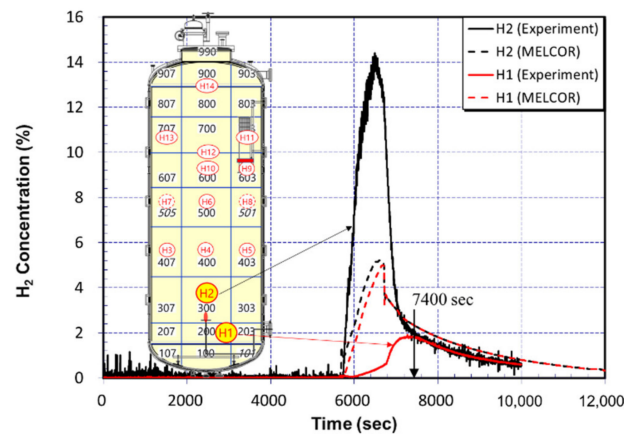


**Figure 13.** Comparison of MELCOR predictions with measurement data for SSP1 test: (a) Relative humidity; (b) Measurement locations.

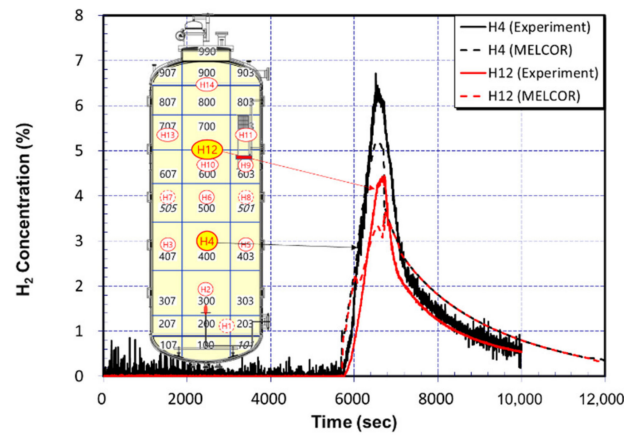
The rapid decrease and increase of humidity around 7000 s in Figure 13 is due to variation of saturation vapor pressure, which can be inferred from gas temperature in Figure 12.

If we see the changes in hydrogen concentration in the SPARC vessel due to the operation of the hydrogen control system, PAR and the spray injection system, as shown in Figure 14, the MELCOR prediction follows the overall trend of increase and decrease of hydrogen concentration, but the following differences can be found:

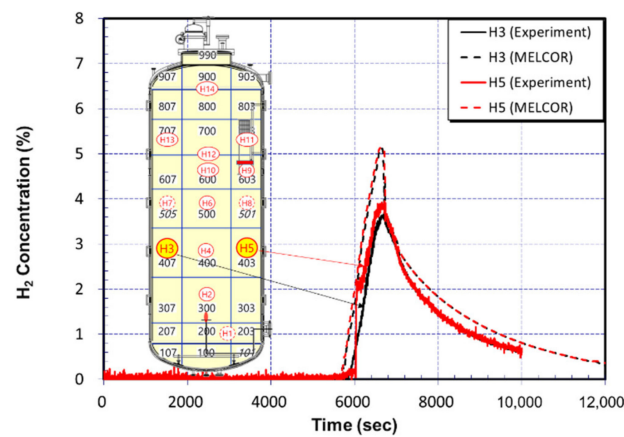
- The measurement of high hydrogen concentration due to the presence of strong hydrogen jets at the elevation near the hydrogen injection tube (H2) is under-predicted by the volume-averaged values of MELCOR prediction as shown in Figure 14a.
- From the test results the hydrogen concentration measurement (H1) at the bottom of the SPARC container (CV 200 area) begins to increase later than other areas because hydrogen fills the upper space first at the time of hydrogen injection. It is approximately after 7400 s that all hydrogen concentrations are uniformly distributed throughout the internal region of the vessel. However, the lumped approach by MELCOR cannot resolve the local distributions in detail.
- The distribution of maximum hydrogen concentration values at each measurement position is not accurately predicted, as shown in Figure 14b,c.



(a)



(b)



(c)

**Figure 14.** Comparison of H<sub>2</sub> concentration for SSP1 test: (a) At locations of H1 and H2; (b) At locations of H4 and H12; (c) At locations of H3 and H5.

## 5. Conclusions

MELCOR simulations of hydrogen mitigation systems in the SPARC test facility operating a PAR and spray system are performed in the present study. For this purpose, a SPARC-SPRAY-PAR (SSP1) experiment is chosen to benchmark the MELCOR predictions against test data.

As part of our efforts to establish a confident environment for MELCOR analysis of the SPARC experiments, we prepared and tested the base input model of the SPARC test vessel by a simple verification problem with well-defined boundary conditions. Furthermore, the implementation of a KNT PAR correlation to the present MELCOR input model is shown to be appropriate.

From the simulation of the experiment, SSP1, the following characteristics of pressure behavior observed from the experiment are well regenerated by MELCOR:

- The linearly increasing rate of pressure by compressing the vessel with steam injection.
- Variation of pressure increase due to hydrogen injection and a PAR actuation.
- Rapid de-pressurization as soon as spray injection starts, and subsequent re-rising and moderate decrease of pressure.

The MELCOR prediction follows the overall trend of an increase and decrease of hydrogen concentration, but the following differences can be found:

- The locally high steam jet cannot be captured by the volume-average calculation of MELCOR.
- Resolution of the hydrogen concentration along different elevations.
- Early prediction of uniform gas mixing.

Since the flow is very complex inside the very large space of actual containment, there is a limitation to simulate effects of spray on the PAR in the small scale of the test facility. However, considering the purpose of the SPARC experiments to more efficiently manage the operation and hydrogen control of PARs through the experimental reproduction of the phenomena we expect, or conversely, the identification of phenomena we do not understand, it will continue to support the verification of analytical models using experimental data and to analyze the impact of spray on PAR operations in severe accident conditions.

**Author Contributions:** Conceptualization, H.T.K. and J.K.; Methodology, H.T.K.; Software, J.K.; Validation, H.T.K., and J.K.; Formal Analysis, H.T.K.; Investigation, H.T.K.; Resources, H.T.K.; Data Curation, H.T.K. and J.K.; Writing—Original Draft Preparation, H.T.K.; Writing—Review & Editing, J.K.; Visualization, H.T.K.; Supervision, J.K.; Project Administration, J.K.; Funding Acquisition, H.T.K. All authors have read and agreed to the published version of the manuscript.

**Funding:** This work was supported by the National Research Foundation of Korea (NRF) grant funded by the Korea government (Ministry of Science, ICT) (No. 2017M2A8A4015277).

**Conflicts of Interest:** The authors declare no conflict of interest. The funders had no role in the design of the study; in the collection, analyses, or interpretation of data; in the writing of the manuscript, and in the decision to publish the results.

## References

1. IAEA. *Mitigation of Hydrogen Hazards in Severe Accidents in Nuclear Power Plants*; IAEA-TECDOC-1661; International Atomic Energy Agency: Vienna, Austria, 2011.
2. Hong, S.-W.; Kim, H.T.; Kim, J. *PAR Experiments in the World and KAERI PAR Experiment*; KAERI/TR-7478/2018; KAERI: Daejeon, Korea, 2018.
3. Bentaib, A.; Meynet, N.; Bleyer, A. Overview on Hydrogen Risk Research and Development Activities: Methodology and Open Issues. *Nucl. Eng. Technol.* **2015**, *47*, 26–32. [[CrossRef](#)]
4. Kim, J.; Hong, S.-H.; Park, K.-H.; Kim, J.-H.; Oh, J.-Y.; Kim, H.T.; Kim, S.B.; Hong, S.-W.; Na, Y.S. *Experimental Study of Hydrogen Behaviors Affected by Pressure Control Systems in a Reactor Containment*; KAERI/TR-7991/2019; KAERI: Daejeon, Korea, 2019.

5. Kim, J.; Kim, H.T. Research on a Hydrogen Stratification Induced by PARs Installed in a Containment. In Proceedings of the Transactions of the Korean Nuclear Society Autumn Meeting, Yeosu, Korea, 24–26 October 2018.
6. Gauntt, R.O.; Cash, J.E.; Cole, R.K.; Erickson, C.M.; Humphries, L.L.; Rodríguez, S.B.; Young, M.F. *MELCOR Computer Code Manuals, Version 1.8.6, Vol. 1: Primer and Users' Guide*; NUREG/CR-6119, Volume 1, Rev. 3, SAND 2005-5713; Sandia National Laboratories: Albuquerque, NM, USA, 2005.
7. Humphries, L.L.; Beeny, B.A.; Gelbard, F.; Louie, D.L.; Phillips, J. *MELCOR Computer Code Manuals, Vol. 2: Reference Manual, Version 2.2.9541*; SAND 2018-13560; Sandia National Laboratories: Albuquerque, NM, USA, 2018.
8. Kim, H.T.; Kim, J. Development of a MELCOR Input for Hydrogen Experiments in the SPARC Test Facility. In Proceedings of the Transactions of the Korean Nuclear Society Autumn Meeting, Yeosu, Korea, 24–26 October 2018.
9. Fischer, K. Qualification of Passive Catalytic Module for Hydrogen Mitigation. *Nucl. Technol.* **1995**, *112*, 58–62. [[CrossRef](#)]
10. Kim, J.; Kim, H.T.; Hong, S.; Park, K.-H.; Kim, J.-H.; Oh, J.-Y. Experimental Study of Hydrogen Behaviors Affected by Pressure Control Systems in a Reactor Containment. In Proceedings of the Transactions of the Korean Nuclear Society Virtual Spring Meeting, Daejeon, Korea, 9–10 July 2020.
11. SOAR on Containment Thermalhydraulics and Hydrogen Distribution. Available online: [https://inis.iaea.org/search/search.aspx?orig\\_q=RN:41041086](https://inis.iaea.org/search/search.aspx?orig_q=RN:41041086) (accessed on 7 September 2020).
12. OECD/NEA Experts. *OECD/SETH-2 Project PANDA and MISTRA Experiments Final Summary Report*; NEA-CSNI-R-2012-5; OECD/NEA: Paris, France, 2012.
13. Paranjape, S.; Mignot, G.; Paladino, D. Effect of thermal stratification on full-cone spray performance in reactor containment for a scaled scenario. In Proceedings of the 22nd International Conference on Nuclear Engineering (ICONE22), Prague, Czech Republic, 7–11 July 2014.
14. Paranjape, S.; Kapulla, R.; Mignot, G.; Paladino, D.; Zboray, R. Light water reactor hollow cone containment spray performance tests in the presence of light non-condensable gas. In Proceedings of the 15th International Topical Meeting on Nuclear Reactor Thermal-Hydraulics (NURETH-15), Pisa, Italy, 12–17 May 2013.
15. Gupta, S.; Langer, G.; Freitag, M.; Colombet, M.; Schmidt, E.; Laufenberg, B. *Hydrogen Combustion during Spray Operation: Tests HD-30 to HD-35*; Technical Report of OECD/NEA THAI-2 Project; 1501420-TR-HD-30–35; Becker Technologies GmbH: Eschborn, Germany, 2014.
16. Kim, J.; Lee, U.; Hong, S.-W.; Kim, S.-B.; Kim, H.-D. Spray effect on the behavior of hydrogen during severe accidents by a loss-of-coolant in the APR1400 containment. *Int. Commun. Heat Mass Transf.* **2006**, *33*, 1207–1216. [[CrossRef](#)]
17. Mimouni, S.; Lamy, J.-S.; Lavieville, J.; Guieu, S.; Martin, M. Modelling of sprays in containment applications with a CMFD code. *Nucl. Eng. Des.* **2010**, *240*, 2260–2270. [[CrossRef](#)]
18. Malet, J.; Blumenfeld, L.; Arndt, S.; Babic, M.; Bentaib, A.; Dabbene, F.; Kostka, P.; Mimouni, S.; Movahed, M.; Paci, S.; et al. Sprays in containment: Final results of the SARNET spray benchmark. *Nucl. Eng. Des.* **2011**, *241*, 2162–2171. [[CrossRef](#)]
19. KNT. PAR. Available online: [http://gbs.gobizkorea.com/catalog/product\\_view.jsp?blogId=kntcom&objId=1102591](http://gbs.gobizkorea.com/catalog/product_view.jsp?blogId=kntcom&objId=1102591) (accessed on 7 September 2020).
20. Park, J.-W.; Koh, B.-R.; Suh, K.Y. Demonstrative testing of honeycomb passive autocatalytic recombiner for nuclear power plant. *Nucl. Eng. Des.* **2011**, *241*, 4280–4288. [[CrossRef](#)]
21. Kim, I.; Kim, D.-S. APR1400: Evolutionary Korean Next Generation Reactor. In Proceedings of the 10th International Conference on Nuclear Engineering (ICONE-10), Arlington, TX, USA, 14–18 April 2002.
22. Kim, C.H.; Sung, J.J.; Ha, S.J.; Seo, P.W. Operational Experience of Ceramic Honeycomb Passive Autocatalytic Recombiner as a Hydrogen Mitigation System. In Proceedings of the 16th International Topical Meeting on Nuclear Reactor Thermal-Hydraulics (NURETH-16), Chicago, IL, USA, 30 August–4 September 2015.
23. Kelm, S.; Jahn, W.; Rinecke, E. Operational Behaviour of Catalytic Recombiners—Experimental Results and Modelling Approaches. In Proceedings of the workshop on Experiments and CFD Code Application to Nuclear Reactor Safety (XCFD4NRS), Grenoble, France, 10–12 September 2008.
24. Bachelier, E.; Arnould, F.; Auglaire, M.; Boeck, B.; Braillard, O.; Eckardt, B.; Ferroni, F.; Moffett, R. Generic Approach for Designing and Implementing a Passive Autocatalytic Recombiner PAR-System in nuclear power plant containments. *Nucl. Eng. Des.* **2003**, *221*, 151–165. [[CrossRef](#)]

25. AREVA Passive Autocatalytic Recombiner. Available online: [http://us.aveva.com/home/liblocal/docs/Solutions/liteature/G-008-V1PB-2011-ENG\\_PAR\\_reader.pdf](http://us.aveva.com/home/liblocal/docs/Solutions/liteature/G-008-V1PB-2011-ENG_PAR_reader.pdf) (accessed on 7 September 2020).
26. Dewit, W.A.; Koroll, G.W.; Sitar, L.; Graham, W.R.C. *Hydrogen Recombiner Development at AECL*; AECL-1172 NEA/CSNI(96)8; AECL: Chalk River, ON, Canada, 1996.
27. Jeon, J.; Choi, W.; Kim, N.K.; Jeun, G.; Kim, S.J. MELCOR Simulation of Containment Spray for Potential Regulation of 100TBq Cesium-137 Release from OPR1000. In Proceedings of the Transactions of the Korean Nuclear Society Spring Meeting, Jeju, Korea, 12–13 May 2016.

**Publisher’s Note:** MDPI stays neutral with regard to jurisdictional claims in published maps and institutional affiliations.



© 2020 by the authors. Licensee MDPI, Basel, Switzerland. This article is an open access article distributed under the terms and conditions of the Creative Commons Attribution (CC BY) license (<http://creativecommons.org/licenses/by/4.0/>).